Radius-independent resonances in electron-hole drop magnetoplasmas

J. R. Dixon, Jr.* and J. K. Furdyna
Department of Physics, Purdue University, West Lafayette, Indiana 47907
(Received 28 August 1978)

We discuss theoretically the microwave and far-infrared spectra which exist in the parameter ranges appropriate to small electron-hole drops in Ge when they are located in a dc magnetic field. Our examination employs the perturbation-theory results of Ford, Furdyna, and Werner, which rigorously describe the interaction of a small gyrotropic sphere with external time-varying electric and magnetic fields. We consider only the two high-symmetry orientations of the dc magnetic field, parallel to the [100] axis of Ge and parallel to the [111] axis of Ge, for which the electron-hole magnetoplasma in Ge is described by a dielectric tensor of a form amenable to the perturbation theory. The theory predicts several radius-independent electric and magnetic resonances. In parameter ranges appropriate to compensated electron-hole drops in Ge, we find that the positions of all resonances are functions only of the various carrier effective masses and ratios of the concentrations of the different carriers. The intensities of the electric resonances are inversely proportional to the electron carrier concentration and vary as the cube of sphere radius and the fourth power of frequency. The intensities of the magnetic resonances are directly proportional to the electron carrier concentration and vary with the fifth power of radius and the square of frequency. We find that two additional electric resonances can occur when the electron-hole drop is uncompensated. The positions of these resonances depend directly upon the difference in the electron and hole carrier densities.

I. INTRODUCTION

Several authors have recently reported complex spectra of well-resolved microwave and far-infrared resonances, associated with electron-hole drops (EHD) in germanium in the presence of an external dc magnetic field.[1-7] These resonances depend directly on the properties of the electron-hole plasma and constitute potentially powerful probes for determining the EHD characteristics.

Unfortunately, a quantitative interpretation of the resonance spectra meets with a serious difficulty: the presence of the dc magnetic field, required by the experiment, makes the electron-hole plasma anisotropic, and the interaction of an electromagnetic wave with a spherical plasma of arbitrary anisotropy remains an unsolved problem of classical electrodynamics. For this reason, much of the discussion of the magnetic-field-dependent microwave resonances in EHD has been, so far, qualitative, using the *ad hoc* phenomenological model of Cardona and Rosenblum[8] as a point of departure.[1,6,9]

Recently, however, Ford, Furdyna, and Werner[10] (FFW) solved the problem of the interaction of an electromagnetic wave with a small[11] gyrotropic sphere, characterized by a complex dielectric tensor of the form

$$\vec{K} = \begin{bmatrix} K_{xx} & K_{xy} & 0 \\ -K_{xy} & K_{xx} & 0 \\ 0 & 0 & K_{zz} \end{bmatrix} \qquad (1)$$

using a perturbation expansion. Their results can be applied directly to the microwave interaction with small EHD for certain field orientations and thus provide, for the first time, a rigorous handle on the problem.[12]

In this paper we use the results of FFW to examine theoretically the spectrum of microwave resonances existent in the parameter ranges appropriate to EHD in germanium when the external magnetic field is applied either along the [100] or the [111] crystallographic axis, the two high-symmetry orientations for which the electron-hole plasma of the droplet is described by a dielectric tensor in the form of Eq. (1). We also restrict attention to "small" droplets, which have radii less than 10 μm,[13-15] in order to satisfy the perturbation criteria of FFW.[11] Specifically, we do not consider the large EHD (the γ drops) observed in inhomogeneously stressed Ge,[6,7] since both their size and the conditions under which they were created preclude their quantitative discussion in the context of the perturbation theory. We approach the problem of resonances in EHD macroscopically, by formulating and examining the electrical and magnetic polarizabilities for normal-mode excitations of the droplets as a function of the applied dc magnetic field. Resonance conditions, linewidths, and intensities are discussed, and both compensated as well as uncompensated electron-hole plasmas are considered. Since the resonance spectra are very complex, particular attention is given to identifying and classifying the resonances according to the microscopic mechanisms which give rise to the various peaks.

II. ELECTRIC RESONANCES

In this section, we discuss the radius-independent resonances that arise from the interaction of a time-varying *electric* field with a magnetoplasma sphere. After describing the appropriate macroscopic formalism, we first review the resonance spectra of magnetoplasma spheres composed of materials with isotropic band structures and then discuss the resonance spectra for EHD in Ge. Throughout this paper, we employ mks units.

A. Macroscopic formalism

We assume that the fields outside the sphere are spatially uniform, i.e., that the wavelength of the electromagnetic radiation in the medium outside the gyrotropic sphere greatly exceeds the sphere radius. We consider separately the three linearly independent modes of excitation of a gyrotropic sphere (denoted by the subscript m) into which an arbitrary time-varying field (electric or magnetic) can be resolved. The modes of excitation consist of two transverse circular polarizations ($m=\pm$), where the time-varying external field is perpendicular to a dc magnetic field $\vec{B}$, and of a longitudinal polarization ($m=\|$), where the time-varying external field is parallel to $\vec{B}$. The gyrotropic tensor, Eq. (1), can be diagonalized in the coordinate system associated with these modes, which is given by the three unit vectors $\hat{e}_m$,

$$\hat{e}_+ = \frac{1}{\sqrt{2}}(\hat{x}+i\hat{y}), \quad \hat{e}_- = \frac{1}{\sqrt{2}}(\hat{x}-i\hat{y}), \quad \hat{e}_\| = \hat{z}, \tag{2}$$

resulting in the form

$$\vec{\kappa} = \begin{bmatrix} \kappa_+ & 0 & 0 \\ 0 & \kappa_- & 0 \\ 0 & 0 & \kappa_\| \end{bmatrix} = \begin{bmatrix} \kappa_{xx}+i\kappa_{xy} & 0 & 0 \\ 0 & \kappa_{xx}-i\kappa_{xy} & 0 \\ 0 & 0 & \kappa_{zz} \end{bmatrix}. \tag{3}$$

The time-averaged power absorbed by a gyrotropic sphere from a time-varying electric field $\vec{E}_m^{ac} e^{-i\omega t}$ is

$$P_m^E = \tfrac{1}{2}\omega\epsilon_0 \operatorname{Im}\alpha_m^E |\vec{E}_m^{ac}|^2, \tag{4}$$

where ω is the angular frequency of the field and $\operatorname{Im}\alpha_m^E$ is the imaginary part of the electric polarizability. According to FFW,[10] the complex electric-dipole polarizability is

$$\alpha_m^E = 2\pi a^3 \frac{[2+\frac{1}{5}\kappa_0(\omega a/c)^2]\kappa_m - 2\kappa_0}{[1-\frac{1}{5}\kappa_0(\omega a/c)^2]\kappa_m + 2\kappa_0}, \tag{5}$$

where κ_0 is the dielectric constant of the medium surrounding the sphere, and a is the sphere radius.

For the situation typical of EHD in Ge ($a \leq 10$ μm, $\kappa_0 = 16$), the dimensional corrections in Eq. (5) may be neglected for the microwave and far-infrared frequencies. Doing so yields the expression

$$\alpha_m^E = 4\pi a^3(\kappa_m - \kappa_0)/(\kappa_m + 2\kappa_0), \tag{6}$$

from which we get

$$\operatorname{Im}\alpha_m^E = 12\pi a^3 \kappa_0 \kappa_m''/[(\kappa_m'+2\kappa_0)^2 + \kappa_m''^2], \tag{7}$$

where prime and double prime indicate the real and imaginary parts of the complex dielectric tensor elements. This expression was first shown to be applicable to the gyrotropic sphere in the Rayleigh limit by Galeener[16] and is identical in form to the Rayleigh limit expression for an isotropic sphere.[17] When the Drude expressions for the dielectric tensor elements are substituted into Eq. (6), it reduces to expressions derived by the depolarization method of Dresselhaus, Kip, and Kittel.[18,19]

When the losses are small ($\kappa_m'' \ll |\kappa_m'|$), the resonance condition is

$$\kappa_m' + 2\kappa_0 = 0. \tag{8}$$

From a cursory inspection of this equation, it is obvious that graphical techniques (i.e., plotting κ_m' and examining its topography for intersections with $-2\kappa_0$) will prove immensely helpful in identifying the circumstances under which resonances will occur.[16,19,20]

B. One- and two-carrier spherical magnetoplasmas

In order to establish a framework in which the radius-independent electric resonances of EHD can be appreciated, we review the electric Rayleigh-limit spectra of one-carrier and compensated, two-carrier spherical magnetoplasmas. Throughout this paper, we employ Drude expressions for the principal dielectric tensor elements (remembering, however, that the macroscopic formulation is not limited to any particular microscopic model for κ_m). For N types of carriers with an isotropic band structure, we have

$$\kappa_\pm = \kappa_l - \sum_{k=1}^{N} \frac{\omega_{pk}^2}{\omega} \frac{\omega \pm \omega_{ck} - i\tau_k^{-1}}{(\omega \pm \omega_{ck})^2 + \tau_k^{-2}} \tag{9}$$

and

$$\kappa_\| = \kappa_l - \sum_{k=1}^{N} \frac{\omega_{pk}^2}{\omega} \frac{\omega - i\tau_k^{-1}}{\omega^2 + \tau_k^{-2}}, \tag{10}$$

where

$$\omega_{pk}^2 = n_k e^2/M_k\epsilon_0, \quad \omega_{ck} = q_k B/M_k, \tag{11}$$

κ_l is the lattice dielectric constant, τ is the carrier relaxation time, n is the free-carrier concentration, M is the carrier effective mass, q is

the carrier charge (including sign), and k is a subscript indicating the kth carrier. Throughout this paper, we will regard the magnetic field B as the quantity that is to be varied experimentally.

For a single-carrier magnetoplasma ($N=1$), the imaginary part of the electric-dipole polarizability, Eq. (6), for the transverse modes of excitation becomes

$$\mathrm{Im}\alpha_{\pm}^{E} = \frac{12\pi a^3 \kappa_0}{(\kappa_l + 2\kappa_0)^2} \frac{\omega_p^2 \tau}{\omega} \times \frac{1}{1+[\omega - \omega_p^2/\omega(\kappa_l+2\kappa_0) \pm \omega_c]^2\tau^2} . \quad (12)$$

The resonance condition is simply

$$\omega_c = \pm[\omega_p^2/\omega(\kappa_l+2\kappa_0) - \omega] . \quad (13)$$

The situation described by this resonance condition was first discussed by Dresselhaus, Kip, and Kittel.[18] When the first term is negligible, i.e., when n is small, resonance occurs when $|\omega_c| = \omega$ for the polarization which has the same sense of rotation as does the cyclotron orbit of the carrier in the magnetic field. We will refer to this polarization as the cyclotron-resonance-active (CRA) polarization. As n increases, the resonance shifts to lower magnetic fields in the CRA polarization. Eventually, the resonance appears in the opposite polarization, which we will refer to as the cyclotron-resonance-inactive (CRI) polarization, at low magnetic fields and moves to higher fields as n increases.

The power absorbed at this resonance is

$$P_{\pm}^{E}(B^{\mathrm{res}}) = \frac{6\pi a^3 \kappa_0 n e^2 \tau}{(\kappa_l+2\kappa_0)^2 M} |\vec{E}_{\pm}^{\mathrm{ac}}|^2 , \quad (14)$$

where B^{res} is the magnetic field at which resonance occurs. Thus, the resonance strength is independent of frequency and is directly proportional to carrier concentration and relaxation time. The line shape of the resonance is Lorentzian in B, having a halfwidth at half power of

$$(\Delta B)_{1/2} = 1/\mu = M/e\tau , \quad (15)$$

where μ is the carrier mobility.

For sphere radii small enough to neglect the dimensional correction terms in the expression for the electric polarizability, a description of the internal electric field requires only FFW's zero-order term in the internal electric field expansion, Eq. (52) of Ref. 10. Thus, the internal electric field $\vec{E}^{\mathrm{int}}$ is uniform throughout the sphere:

$$\vec{E}_m^{\mathrm{int}} = [3\kappa_0/(2\kappa_0+\kappa_m)]\vec{E}_m^{\mathrm{ac}} . \quad (16)$$

Since the internal free current density is also uniform, the time-averaged power absorbed by the sphere can be written as

$$P_m^E = \tfrac{1}{2} V \mathrm{Re}(\vec{j}_m^{\mathrm{int}} \cdot \vec{E}_m^{\mathrm{int}*}) = \tfrac{2}{3}\pi a^3 \epsilon_0 \omega \kappa_m'' |\vec{E}_m^{\mathrm{int}}|^2 , \quad (17)$$

where j_m^{int} is the internal free current density, V is the sphere volume, and

$$|\vec{E}_m^{\mathrm{int}}| = \frac{3\kappa_0}{[(\kappa_m'+2\kappa_0)^2 + \kappa_m''^2]^{1/2}} |\vec{E}_m^{\mathrm{ac}}| . \quad (18)$$

An examination of Eqs. (17) and (18) points to the conclusion that the single-carrier resonance, as well as all other electric resonances which might exist, occurs in the term $|\vec{E}_m^{\mathrm{int}}|$, i.e., it is due to buildup of the internal electric field at the resonance condition (8) rather than any increase in absorption associated with the inherent behavior of κ_m''. As shown in Eq. (18), $|\vec{E}_m^{\mathrm{int}}|$, in general, is reduced by the factor $3\kappa_0/|2\kappa_0+\kappa_m|$. Thus, at the *cyclotron*-resonance field, where $|\kappa_m'| \to \infty$, the internal field is screened out by the surface charge so that a resonance does not occur at that point.

In the case of the longitudinal model of excitation, no resonances occur because $\kappa_{\parallel}$ is independent of magnetic field for any isotropic system, one or two carrier. Furthermore, if the relaxation times for both carriers are large, there are also no microwave or far-infrared resonances for the transverse mode of excitation for a compensated, two-carrier system when the carrier density n is in the range characteristic of EHD (~10^{17} cm^{-3}). Specifically, utilizing lossless expressions for $\kappa_{\pm}'$, we find that no resonances exist if

$$n > \epsilon_0(\kappa_l+2\kappa_0)(M_e+M_h)\omega^2/4e^2 , \quad (19)$$

where the subscripts e and h indicate electrons and holes, respectively. At 35 GHz, with parameters similar to those of EHD in Ge ($\kappa_0=\kappa_l=16$; $M_e = 0.135M_0$; $M_h = 0.277M_0$, where M_0 is the free-electron mass), this demarcation point occurs at $n = 7.5\times10^{13}$ cm^{-3}.

C. Resonances in EHD in germanium

In this section, we consider the resonance spectrum for EHD magnetoplasmas in Ge. As stated before, we limit ourselves to the two high-symmetry directions, $\vec{B}\|[100]$ and $\vec{B}\|[111]$, for which the dielectric tensor has the form of Eq. (1). For simplicity, we assume that the light- and heavy-hole bands are isotropic. The carrier densities used will be such that $n = n_e = n_{\mathrm{lh}} + n_{\mathrm{hh}}$, $n_{\mathrm{lh}} = \frac{1}{20} n_e$, and $n_{\mathrm{hh}} = \frac{19}{20} n_e$, where the subscripts e, lh, and hh indicate the conduction, light-hole, and heavy-hole bands, respectively.

With $\vec{B}\|[100]$, the expressions for the principal dielectric tensor elements are[20]

$$\kappa_{\pm} = \kappa_l - \frac{\omega_{pe}^2}{\omega}\frac{\omega + i\nu_e \pm \omega_1}{(\omega + i\nu_e)^2 - \omega_{ce}^2} - \frac{\omega_{p\,\mathrm{hh}}^2}{\omega}\frac{\omega + i\nu_{\mathrm{hh}} \mp \omega_{c\,\mathrm{hh}}}{(\omega + i\nu_{\mathrm{hh}})^2 - \omega_{c\,\mathrm{hh}}^2} - \frac{\omega_{p\,\mathrm{lh}}^2}{\omega}\frac{\omega + i\nu_{\mathrm{lh}} \mp \omega_{c\,\mathrm{lh}}}{(\omega + i\nu_{\mathrm{lh}})^2 - \omega_{c\,\mathrm{lh}}^2} \quad (20)$$

and

$$\kappa_{\parallel} = \kappa_l - \frac{\omega_{pe}^2}{\omega(\omega + i\nu_e)}\frac{(\omega + i\nu_e)^2 - \omega_2^2}{(\omega + i\nu_e)^2 - \omega_{ce}^2} - \frac{\omega_{p\,\mathrm{hh}}^2}{\omega(\omega + i\nu_{\mathrm{hh}})} - \frac{\omega_{p\,\mathrm{lh}}^2}{\omega(\omega + i\nu_{\mathrm{lh}})}\,, \quad (21)$$

where

$$\omega_{pe}^2 = \frac{ne^2}{3\epsilon_0}\left(\frac{1}{M_L} + \frac{2}{M_T}\right) = \frac{ne^2}{\epsilon_0 M_{pe}}\,, \quad (22)$$

$$\omega_{ce}^2 = \frac{e^2B^2}{3M_T}\left(\frac{2}{M_L} + \frac{1}{M_T}\right) = \frac{e^2B^2}{M_{ce}^2}\,, \quad (23)$$

$$\omega_1 = \frac{eB}{M_T}\frac{(2M_T + M_L)}{(M_T + 2M_L)} = \frac{eB}{M_1}\,, \quad (24)$$

$$\omega_2^2 = \frac{3e^2B^2}{M_T(M_T + 2M_L)} = \frac{e^2B^2}{M_2^2}\,, \quad (25)$$

$\nu = 1/\tau$, M_L and M_T are the longitudinal and transverse electron effective masses, and the subscripts e, lh, and hh indicate electron, light-hole, and heavy-hole parameters. As previously mentioned, graphs of the real part of these expressions in the lossless limit ($\nu \to 0$) have proven useful in locating resonances because of the ease of identifying those points at which the resonance condition (8) is satisfied. Figure 1 displays the real part of each of the principal dielectric tensor elements, Eqs. (20) and (21), for parameters appropriate to EHD, and Fig. 2 shows the corresponding resonance spectra. In performing these calcula-

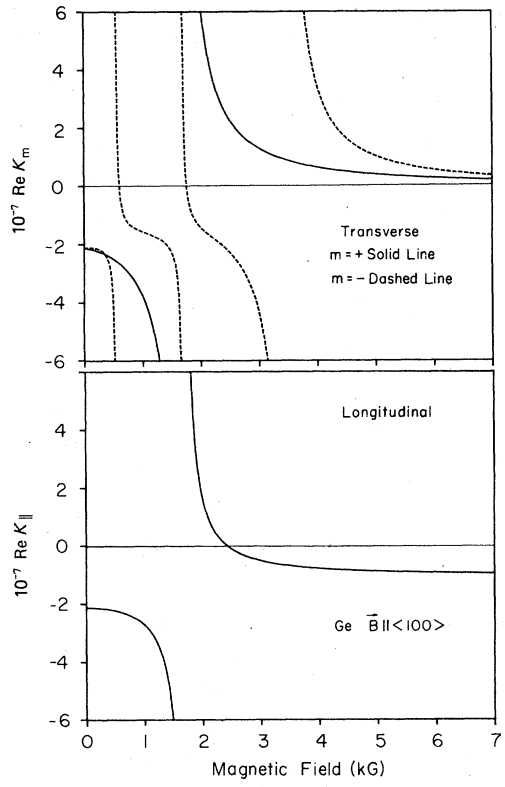

FIG. 1. Real part of the principal dielectric tensor elements κ_m' as a function of magnetic field for $\vec{B}$ parallel to the [100] crystallographic axis of Ge. The parameters used in the calculation were $n = 2.5 \times 10^{17}$ cm^{-3}, $\tau_e = \tau_{\mathrm{hh}} = \tau_{\mathrm{lh}} \to \infty$, $\kappa_l = \kappa_0 = 16$, and $\omega/2\pi = 35$ GHz. The effective masses and ratios of the concentrations of light and of heavy holes to electrons are given in the text. Because of the large range of κ_m', the intersection of κ_m' with the abscissa suffices for the accurate location of the electric resonances shown in Fig. 2.

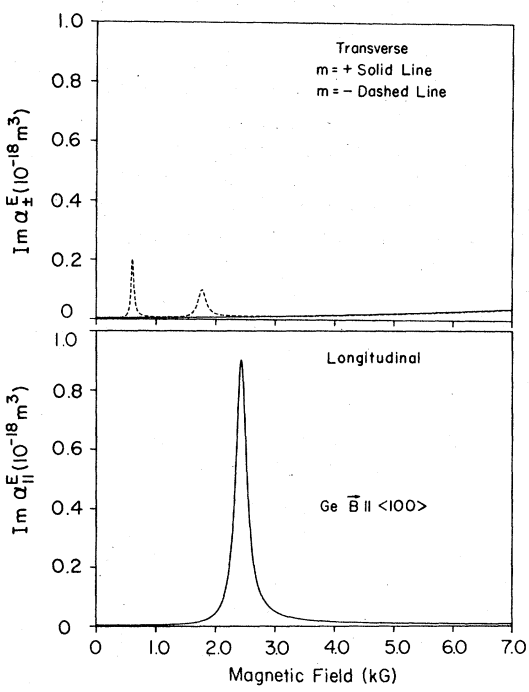

FIG. 2. Imaginary part of the electric polarizability for the three modes of excitation of a gyrotropic sphere as a function of magnetic field, for the case of Ge with $\vec{B}$ along the [100] crystallographic axis. The radius of the sphere was 3 μm, and the material parameters employed in the calculation are listed in the caption to Fig. 1, except that $\tau_e = \tau_{\mathrm{hh}} = \tau_{\mathrm{lh}} = 10^{-10}$ sec.

tions, we took $n=2.5\times10^{17}$ cm^{-3} and used the bulk germanium carrier effective masses[21]: $M_L=1.59M_0$, $M_T=0.082M_0$,[22] $M_{lh}=0.043M_0$, and $M_{hh}=0.28M_0$.[23] A quick comparison of Figs. 1 and 2 shows that the resonance positions are located accurately via the plots shown in Fig. 1.

The low-field resonance in the transverse polarization in Fig. 2 is produced by the introduction of the third carrier species in Eq. (20). Assuming, for the moment, that the electron band is isotropic with $M_e=M_{ce}=0.135M_0$, the resonance condition (8) and Eq. (9) yield, in the lossless limit, an expression for the resonance position

$$B_{\pm}^{\rm res}=\mp\frac{\omega}{e}\,\frac{M_{lh}(\gamma_{hh}M_e+M_{hh})+\gamma_{lh}M_{hh}M_e}{M_e+\gamma_{hh}M_{hh}-(1+\gamma_{hh})M_{lh}}\,, \tag{26}$$

valid for the high-carrier-concentration limit, i.e., for $\omega_{pe}\gg\omega(\kappa_l+2\kappa_0)^{1/2}$ where $\gamma_{lh}=n_{lh}/n$ and $\gamma_{hh}=n_{hh}/n$. Where $\gamma_{lh}\ll1$ and $M_{lh}\ll M_{hh}$, Eq. (26) reduces to the form

$$B_{-}^{\rm res}\simeq\omega M_{lh}/e\,. \tag{27}$$

Thus, the resonance introduced by the presence of the third carrier is near the cyclotron-resonance field of the light hole. The introduction of the anisotropy of the electron band tends to move the resonance even closer to the light-hole cyclotron-resonance field.

Both the high-field resonance in the transverse polarization and the resonance in the longitudinal configuration are consequences of the anisotropy in the electron-band structure. The longitudinal resonance is a tilted orbit resonance,[24] i.e., a resonance resulting from the carrier having a component of its cyclotron motion periodic along the field axis. All three resonances shown in Fig. 2 are hybrid resonances,[24] since the resonance positions depend upon the effective masses of more than one carrier species. However, for the situation under consideration, the carrier parameters are such that the resonance fields for the two transverse resonances are determined mainly by one carrier type, the light hole in the case of the low-field resonance [Eq. (27)] and the electron in the case of the high-field resonance.

The behavior of the high-field transverse resonance is made clear when the third carrier type in Eq. (20), the light hole, is neglected. Then the position of that resonance, in the lossless limit, is

$$B_{-}^{\rm res}\simeq\frac{\omega M_1}{e}\,\frac{M_h+M_{pe}}{M_h+M_1}\,, \tag{28}$$

provided that $\omega_{pe}\gg(\kappa_l+2\kappa_0)^{1/2}\omega$. Since M_h is larger than both M_{pe} and M_1, and M_{pe} and M_1 are of nearly the same magnitude ($M_{pe}/M_1\simeq0.8$), the resonance position is determined almost exclusively by M_1, i.e.,

$$B_{-}^{\rm res}\simeq\frac{\omega M_1}{e}=\frac{\omega}{e}M_T\,\frac{M_T+2M_L}{2M_T+M_L}\,. \tag{29}$$

The hybrid character of the longitudinal resonance is evident in the expression for the resonance field

$$B_{\parallel}^{\rm res}=(\omega/e)(M_TM_{100})^{1/2}\,, \tag{30}$$

where

$$M_{100}=\frac{M_T+2M_L+3M_LM_T(\gamma_{lh}/M_{lh}+\gamma_{hh}/M_{hh})}{3+(2M_T+M_L)(\gamma_{lh}/M_{lh}+\gamma_{hh}/M_{hh})}\,. \tag{31}$$

The expression is derived by use of the resonance condition (8) and Eq. (21) in the lossless limit and assumption of the high-carrier-concentration limit, i.e., that $\omega_{plh}^2+\omega_{phh}^2\gg(\kappa_l+2\kappa_0)\omega^2$.

When losses are small, the power absorbed at resonance can be written as

$$P_m^E(B^{\rm res})=(6\pi a^3\kappa_0\epsilon_0\omega/\kappa_m'')|\vec{\mathbf{E}}_m^{\rm ac}|^2\,. \tag{32}$$

In the case of the longitudinal resonance, the small-loss limit ($\omega^2-\omega_2^2\gg\nu_e^2$, $\omega^2-\omega_{ce}^2\gg\nu_e^2$, $\omega^2\gg\nu_{lh}^2$, $\omega^2\gg\nu_{hh}^2$) yields

$$P_{\parallel}^E(B^{\rm res})=(6\pi\kappa_0\epsilon_0^2a^3\omega^4/ne^2)f_{\parallel}|\vec{\mathbf{E}}_{\parallel}^{\rm ac}|^2\,, \tag{33}$$

where $f_{\parallel}$ is a function of relaxation times and ef-

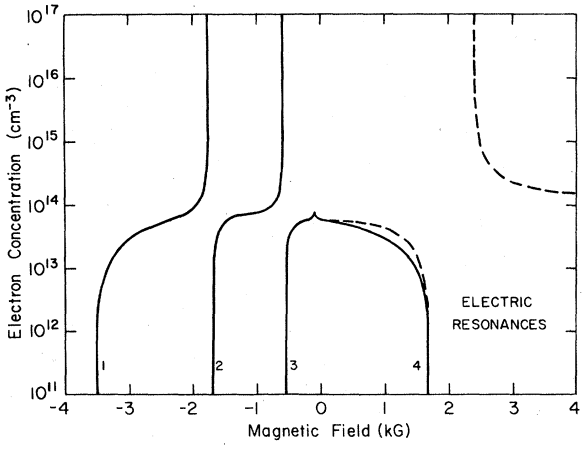

FIG. 3. Field positions of the electric resonances in a 1-μm radius magnetoplasma sphere as a function of carrier concentration. The resonances in the (–) circular polarization are plotted on the negative side of the field axis. The positions of the transverse resonances are plotted with a solid line while the position of the longitudinal resonance is plotted as a dashed line. $\vec{B}$ is parallel to the Ge [100] axis, and the material parameters for the sphere are described in the caption of Fig. 2. The high-carrier-density regime lies above a carrier density of 5×10^{14} cm^{-3} while the low-carrier-density, or cyclotron-resonance, regime lies below 10^{13} cm^{-3}. Note that the resonance positions are independent of carrier concentration in both of these regions.

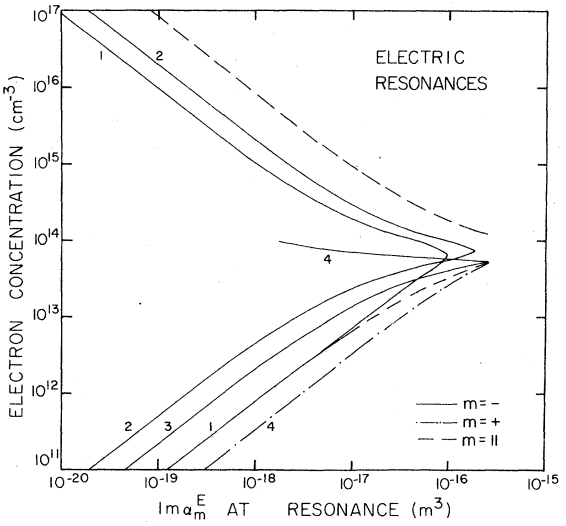

FIG. 4. Imaginary part of the electric polarizability at resonance for the electric resonances as a function of carrier concentration. The numbers 1–4 indicate the corresponding resonances labeled 1–4 in Fig. 3. The solid line marked 4 terminates because it merges into the background absorption at that point. These calculations were done for the same system as was described in the caption of Fig. 3. Note that the resonance strengths are increasing with decreasing n in the high-carrier-concentration region and increasing with increasing n in the low-carrier-concentration region.

fective masses alone. Thus the strength of the longitudinal resonance is proportional to the third power of radius and the fourth power of frequency and, surprisingly, inversely proportional to the carrier concentration.[25]

This behavior is characteristic of *all* electric resonances in compensated magnetoplasmas in the high-carrier-concentration regime (the region appropriate to EHD at microwave and submillimeter wavelengths), where $\omega_{pe} \gg (\kappa_l + 2\kappa_0)^{1/2}\omega$, $\omega_{plh} \gg (\kappa_l + 2\kappa_0)^{1/2}\omega$, and $\omega_{phh} \gg (\kappa_l + 2\kappa_0)^{1/2}\omega$. This can be seen as follows. Figure 3 shows that, in the high-concentration regime, the resonance field positions are independent of n. From Eq. (32), we find that the resonance strength is inversely proportional to κ_m'' and that, since the resonance-field is independent of n, κ_m'' is proportional to n at a given resonance. Thus all electric resonances in the high-carrier-density regime vary *inversely* with n, as shown in Fig. 4. The low-carrier-density, or cyclotron-resonance, region, where $\omega_{pe} \ll (\kappa_l + 2\kappa_0)^{1/2}\omega$, $\omega_{plh} \ll (\kappa_l + 2\kappa_0)^{1/2}\omega$ and $\omega_{phh} \ll (\kappa_l + 2\kappa_0)^{1/2}\omega$, is clearly visible in Figs. 3 and 4. The resonance positions in this regime are also independent of n, but their strengths are proportional to n (see Fig. 4).

The intensities of all electric resonances in compensated magnetoplasmas also depend upon the third power of radius and the fourth power of frequency. Since the resonance-field positions are independent of radius, the third-power dependence of resonance strength on radius is obvious. The variation of the resonance strength with the fourth power of frequency depends upon the fact that the resonance-field positions are directly proportional to ω. In the small-loss limit the denominator of Eq. (32), κ_m'', at resonance is inversely proportional to the cube of frequency, resulting in the expression for the resonance strength, Eq. (32), having the ω^4 behavior. In the cyclotron-resonance region, the resonance strengths depend on the cube of radius but do not depend on frequency, just as in the isotropic single-carrier situation.

Figure 4 shows that the longitudinal resonance does not exist for a certain range of carrier concentrations due to a gap in $\kappa_{\|}'$ produced by the electron-band anisotropy. Finally, in Fig. 5 we demonstrate the validity of the comments we previous-

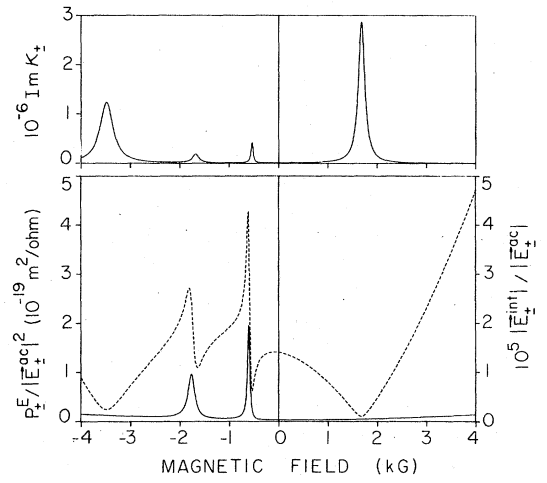

FIG. 5. Imaginary part of the principal transverse dielectric tensor elements κ_m'' (top), the power absorbed from a transverse electric field (bottom, solid line), and the magnitude of the internal electric field (bottom, dashed line) as a function of magnetic field. These quantities are calculated for a 3-μm-radius sphere with the material parameters described in the caption of Fig. 2. The (−) circular polarization is plotted on the negative field axis. The absorbed power peaks do not coincide with the peaks in κ_m'' but occur at the same fields as the internal electric field maxima. Also, the magnitude of the internal electric field has minima at the fields at which κ_m'' has maxima, thus suppressing any peaks in the absorbed power at the cyclotron-resonance fields of the carriers.

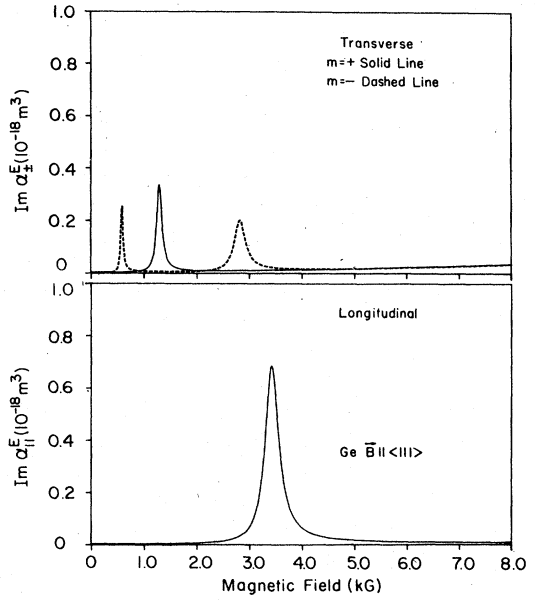

FIG. 6. Imaginary part of the electric polarizability for the three modes of excitation of a gyrotropic sphere as a function of magnetic field for the case of Ge with $\vec{B}$ parallel to the [111] axis. The sphere parameters are identical to those used for Fig. 3, with the exception that different light- and heavy-hole effective masses were used, as described in the text.

ly made in connection with Eqs. (17) and (18). Figure 5 shows that, for the system under discussion, resonances in the absorbed power arise from an enhancement of the internal field. The peaks in κ_m'' are not correlated with the resonance structure of the absorption spectrum.

Figure 6 shows the electric resonance spectra for $\vec{B} \| [111]$ crystallographic axis, with $n = 2.5 \times 10^{17}$ cm^{-3}, $M_{lh} = 0.041 M_0$, and $M_{hh} = 0.376 M_0$.[23] A fourth resonance is present in this spectrum. It arises because, with $\vec{B} \| [111]$, there are now two sets of nonequivalent ellipsoids in the band structure. One ellipsoid has its major axis along the field direction; the other three ellipsoids are equivalent and tilted at an acute angle with respect to $\vec{B}$. The effect of the carriers associated with the single ellipsoid aligned with $\vec{B}$ is much like the introduction of a fourth type of carrier—an isotropic negatively charged one. The resonance produced by the carriers associated with this ellipsoid appears in the transverse (+) polarization (the CRA polarization for electrons) and is a hybrid resonance, its position, for the most part, depending upon the various electron effective masses. The remaining resonances are of the same general character as their [100] counterparts.

D. Resonances in an uncompensated EHD magnetoplasma

When a multiple-carrier system is uncompensated, two additional resonances may appear in the transverse polarizations. This is demonstrated in Fig. 7, where $\kappa_{\pm}'$ for an uncompensated isotropic two-carrier plasma satisfies the resonance condition (8) at two fields. These resonances will occur at magnetic fields larger than the cyclotron-resonance fields.

In the case of an isotropic two-carrier system where $|\omega_{ci}| \gg \omega \gg \tau_i^{-1}$ for $i = e$ and h, the real part of the principal dielectric tensor elements can be written as

$$\kappa_{\pm}' = \kappa_l + \frac{n_e M_e + n_h M_h}{\epsilon_0 B^2} \pm \frac{e}{\epsilon_0 \omega B}(n_e - n_h). \qquad (34)$$

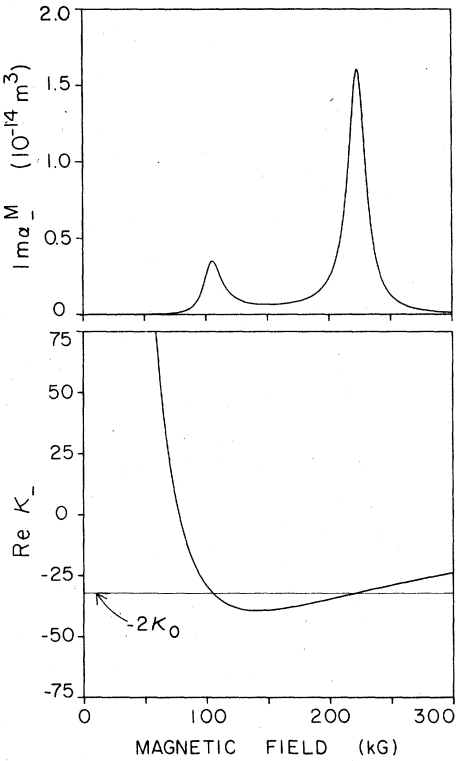

FIG. 7. Imaginary part of the electric polarizability (top) and the real part of the lossless dielectric tensor element (bottom) for the $m = (-)$ polarization. The 3-μm-radius magnetoplasma sphere is an uncompensated two-carrier system in a Ge lattice ($\kappa_l = \kappa_0 = 16$) with parameters: $n_e = 2.69 \times 10^{17}$ cm^{-3}, $n_h = 2.5 \times 10^{17}$ cm^{-3}, $M_e = 0.135 M_0$, $M_h = 0.28 M_0$, $\tau_e = \tau_h = 10^{-10}$ sec, and $\omega/2\pi = 35$ GHz. The horizontal line at -32 (bottom) intersects with κ_-' at the field positions of the two resonances shown in the top half of the figure. Note that with essentially the same parameters the two resonances shown are four orders of magnitude larger than the electric resonances in the compensated EHD magnetoplasmas.

When, additionally, $\omega_{pi} \gg (\kappa_l + 2\kappa_0)^{1/2} |\omega_{ci}|$ for $i = e$ and h, κ_l may be neglected so that the resonance condition is $\kappa'_\pm \simeq 0$. Then it is apparent that the first resonance occurs at the field point at which the principal dielectric tensor element changes from being dominated by the Alfvén term (the second term on the right-hand side) at low fields to being described at higher fields by a heliconlike term (the third term), which has an effective carrier concentration equal to $n_e - n_h$. The field position of this first resonance is then

$$B_\pm^{\rm res} = \mp \frac{\omega}{e} \frac{n_e M_e + n_h M_h}{n_e - n_h} . \tag{35}$$

The resonance always occurs in the CRI polarization of the carrier with the larger carrier density. In the large-carrier-density regime, the power absorbed at resonance is

$$P_\pm^E(B^{\rm res}) = \frac{6\pi a^3 \kappa_0 \epsilon_0^2 \omega^2 (B_\pm^{\rm res})^2}{n_e \nu_e M_e + n_h \nu_h M_h} |\vec{E}_\pm^{\rm ac}|^2$$
$$= \frac{6\pi a^3 \kappa_0 \epsilon_0^2 \omega^4 (n_e M_e + n_h M_h)^2}{(n_e \nu_e M_e + n_h \nu_h M_h)(n_e - n_h)^2} |\vec{E}_\pm^{\rm ac}|^2 . \tag{36}$$

Thus, the strength of the first resonance varies with the third power of radius and the fourth power of frequency, as do all of the previously discussed electric resonances for multiple-carrier magnetoplasmas. However, the resonance strength is inversely proportional to the difference in the carrier densities and, in a sense, directly proportional to the sum of the individual carrier concentrations. In the case of Ge with $\vec{B}$ parallel to the [100] axis and $\omega_{pi}/\sqrt{\kappa_l} \gg |\omega_{ci}| \gg \omega \gg \nu_i$, where $i = e$, lh, and hh, this resonance occurs when[19]

$$B_\pm^{\rm res} = \mp \frac{\omega}{e} \frac{M_l n_e + M_{\rm lh} n_{\rm lh} + M_{\rm hh} n_{\rm hh}}{n_e - n_{\rm lh} - n_{\rm hh}} . \tag{37}$$

At sufficiently large fields, the Alfvén term in Eq. (34) can be neglected. At these high fields, a second resonance is predicted at the field

$$B_\pm^{\rm res} = \mp (n_e - n_h) e / (\kappa_l + 2\kappa_0) \epsilon_0 \omega . \tag{38}$$

Its resonance strength is

$$P_\pm^E(B^{\rm res}) = \frac{6\pi a^3 \kappa_0 \epsilon^2 (n_e - n_h)^2}{(\kappa_l + 2\kappa_0)^2 (n_e M_e \nu_e + n_h M_h \nu_h)} |\vec{E}_\pm^{\rm ac}|^2 . \tag{39}$$

Thus, in contrast to the first resonance, the strength of the resonance now varies as the square of the difference in the carrier concentrations but is roughly inversely proportional to the sum of the carrier densities. Note that Eq. (39) transforms to Eq. (14) as n_h or n_e approaches zero.

It can be shown from Eqs. (8) and (9) that, for a two-carrier isotropic system, the resonances can only occur when the condition

$$n_e \geq \frac{\omega^2 \epsilon_0 (\kappa_l + 2\kappa_0)(M_e + M_h)}{e^2 (1 - n_h/n_e)} . \tag{40}$$

is satisfied. Therefore, the slight charge on EHD in pure Ge (see Refs. 26, 27) would not produce any resonances at microwave or far-infrared frequencies. However, the resonances discussed in this section should be observable for EHD in doped Ge, where the electron and hole carrier densities are believed to differ by the uncompensated impurity concentration.[28] These resonances are highly sensitive to the difference in electron and hole concentrations, thus providing a valuable tool for investigating the effect of doping on EHD.

III. MAGNETIC RESONANCES

In this section, we discuss the radius-independent resonances that arise from the interaction of a time-varying *magnetic* field with a magnetoplasma sphere. We first discuss the macroscopic formalism developed by FFW.[10] Then we apply the formalism to develop a description of the resonance spectra of magnetoplasma spheres consisting of materials with isotropic band structures. We then move to a discussion of the resonance spectra of EHD in Ge.

A. Macroscopic description

As in the case of a time-varying electric field, any time-varying magnetic field can be resolved into three components: two opposite circular polarizations transverse to $\vec{B}$ ($m = \pm$) and one longitudinal with $\vec{B}$ ($m = \|$). The mean power absorbed from any of the normal-mode components of the time-varying magnetic field, $B_m^{\rm ac} e^{-i\omega t}$, by a plasma sphere having a magnetic dipole moment $\vec{M}$ and a magnetic dipole polarizability α^M is

$$P_m^M = \tfrac{1}{2} \omega {\rm Im} (\vec{M}_m \cdot \vec{B}_m^{\rm ac}) = (\omega/2\mu_0) {\rm Im}\, \alpha_m^M |\vec{B}_m^{\rm ac}|^2 , \tag{41}$$

where, according to FFW,[10] the magnetic dipole polarizability is

$$\alpha_m^M = \frac{2\pi}{15} \frac{a^5 \omega^2}{c^2} \frac{\tilde{\kappa}_m}{1 - \frac{2}{21} (\omega a/c)^2 \tilde{\kappa}_m} . \tag{42}$$

Here,

$$\tilde{\kappa}_\pm = \frac{2\kappa_\pm \kappa_{zz}}{\kappa_\pm + \kappa_{zz}} ; \quad \tilde{\kappa}_\| = \frac{2\kappa_+ \kappa_-}{\kappa_+ + \kappa_-} . \tag{43}$$

More explicitly,

$$\tilde{\kappa}'_\pm{}'' = 2 \frac{\kappa'_\pm{}'' |\kappa_{zz}|^2 + \kappa'_{zz}{}'' |\kappa_\pm|^2}{(\kappa'_\pm + \kappa'_{zz})^2 + (\kappa''_\pm + \kappa''_{zz})^2} \tag{44}$$

and

$$\tilde{\kappa}'_\|{}'' = 2 \frac{\kappa'_+{}'' |\kappa_-|^2 + \kappa'_-{}'' |\kappa_+|^2}{(\kappa'_+ + \kappa'_-)^2 + (\kappa''_+ + \kappa''_-)^2} . \tag{45}$$

In this section, our attention will be focused on the small-size limit[11] in which magnetic resonances exist that have radius-indpendent resonance positions.[29] This is a more severe limitation on radius than is involved in ignoring the dimensional corrections in the case of the electric interaction. If we consider only spheres of radii $\lesssim 3$ μm for microwave and submillimeter wavelengths, the radius-dependent correction terms in Eq. (42) can be neglected so that

$$\alpha_m^M = \tfrac{2}{15}\pi(a^5\omega^2/c^2)\tilde{\kappa}_m . \tag{46}$$

The mean absorbed power can then be written as

$$P_m^M = \tfrac{1}{15}\pi\epsilon_0 a^5\omega^3\tilde{\kappa}_m''|\vec{B}_m^{ac}|^2 . \tag{47}$$

An examination of Eqs. (44) and (45) indicates that, should

$$\kappa_+' + \kappa_{zz}' = 0 \tag{48}$$

for the $m=\pm$ mode or

$$\kappa_+' + \kappa_-' = 0 \tag{49}$$

for the $m=\|$ mode of excitation, a resonance will appear in the power absorption of a sphere. Such conditions are analogous to the $\kappa_m' + 2 = 0$ resonance condition for the electric interaction with a small magnetoplasma sphere.

B. Carrier systems with isotropic band structure

1. Single carrier

In the case of a single type of carrier with an isotropic band structure, one resonance occurs in the CRA transverse polarization. Within the context of the Drude model, such a resonance will be Lorentzian in B when the free-carrier term is much greater than the lattice dielectric constant. With κ_l ignored ($\omega_p^2 \gg \kappa_l\omega|\omega_c|$), Eqs. (44) and (46) yield

$$\mathrm{Im}\alpha_\pm^M = \frac{8\pi}{15}\, a^5\, \frac{ne^2\mu_0\omega}{M}\, \frac{\tau^{-1}}{(2\omega \pm \omega_c)^2 + 4\tau^{-2}} . \tag{50}$$

The resonance, occurring when

$$B_\pm^{res} = \mp 2\omega M/q , \tag{51}$$

has a halfwidth at half power of $2/\mu$, which, for the same carrier parameters, is twice that of a single-carrier plasma-shifted cyclotron resonance [Eq. (13)]. The resonance loses its exact Lorentzian form and its position shifts as the contribution of κ_l to Eq. (9) becomes significant compared to the free-carrier term.

The power absorbed at this resonance is

$$P_\pm^M(B^{res}) = \tfrac{1}{15}\pi(ne^2\omega^2a^5/M)\tau\,|\vec{B}_\pm^{ac}|^2 . \tag{52}$$

Thus the resonance strength increases as the fifth power of radius, a characteristic of all magnetic radius-independent resonances, and as the square of the frequency, whereas the resonance strength of the single-carrier plasma-shifted cyclotron resonance was independent of frequency and varied with the third power of radius. Also, the resonance strength of the magnetic resonance is directly proportional to both the carrier concentration and the relaxation time.

No resonance exists for the longitudinal mode of excitation; but a low-field shoulder[10,30] due to the longitudinal magnetic field exists when κ_l is nonnegligible compared to the free-carrier term of the dielectric tensor elements, Eq. (9). When κ_l can be ignored, the longitudinal mode of excitation has no field dependence within the framework of the Drude model since

$$\mathrm{Im}\alpha_\|^M = \frac{2\pi}{15}\, a^5\, \frac{ne^2\mu_0\omega}{M}\, \frac{\tau^{-1}}{\omega^2+\tau^{-2}} . \tag{53}$$

2. Compensated carriers with isotropic band structure

A compensated plasma sphere composed of equal concentrations n of electrons (e) and holes (h) with isotropic band structures has a magnetic resonance for each of the linearly independent modes of excitation. Neglecting $\kappa_l(\omega_{pi} \gg \sqrt{\kappa_l}\,\omega)$ and utilizing the lossless expressions for the dielectric tensor elements, the resonance condition (48) yields the resonance fields:

$$B_\pm^{res} = \frac{\omega}{2e}\Big|M_e - M_h \pm (M_e+M_h) \times [1 + 4M_eM_h/(M_e+M_h)^2]^{1/2}\Big| . \tag{54}$$

If, say, $M_h \gg M_e$, then the square root in Eq. (54) can be expanded to yield

$$B_\pm^{res} \simeq \begin{cases} \dfrac{\omega}{e}\left(M_e + \dfrac{M_eM_h}{M_e+M_h}\right) \simeq 2\,\dfrac{\omega M_e}{e}, & m=+ \\ \dfrac{\omega}{e}\left(M_h + \dfrac{M_eM_h}{M_e+M_h}\right) \simeq \dfrac{\omega}{e}(M_h+M_e), & m=- . \end{cases} \tag{55}$$

Each resonance is associated with one of the two transverse circular polarizations of the time-varying magnetic field. In this case, one resonant field occurs in the CRA polarization for electrons ($m=+$) while the other resonance field occurs in the CRA polarization for holes. An examination of Eq. (55) shows that the resonance associated with each carrier occurs when $|\omega_c| < 2\omega$. Thus, introduction of a second carrier having the same carrier concentration as the first results in the two magnetic resonances being moved closer to their cyclotron resonance fields. When the two carriers have substantially different effective masses, the

shift of the magnetic resonance toward the cyclotron-resonance field is significantly greater for the carrier with the heavier mass.

For the longitudinal field configuration, a hybrid resonance exists which depends on the existence of both carriers. Again neglecting κ_l, the resonance condition (49) yields the resonance field:

$$B_{\parallel}^{\text{res}} = \sqrt{M_e M_h}\ \frac{\omega}{e}\ . \tag{56}$$

When $\omega_{pi}/\sqrt{\kappa_l} \gg \omega \gg \tau_i^{-1}$, where $i = e$ and h, the power absorbed at resonance for this longitudinal resonance is

$$P_{\parallel}^{M}(B^{\text{res}}) = \frac{\pi}{30}\, d^5 \omega^2 n e^2\, \frac{M_e^{-1} + M_h^{-1}}{\tau_e^{-1} + \tau_h^{-1}}\, |\vec{B}_{\parallel}^{\text{ac}}|^2\ . \tag{57}$$

In the regime where $\omega \gg \tau^{-1}$ for all carriers and $\omega_{pe} \gg \sqrt{\kappa_l}\,\omega$ (conditions satisfied by the EHD parameters), the behavior of the longitudinal resonance strength with respect to radius, frequency, and carrier concentration is the same as that of all the magnetic resonances which we shall consider. The magnetic-resonance-field positions are independent of radius and, if κ_l can be ignored, carrier concentration. Consequently, the dependence of resonance strength on the fifth power of radius is obvious. Likewise, since the absorbed power [Eq. (47)] is directly proportional to $\tilde{\kappa}_m''$ and since $\tilde{\kappa}_m''$, within the stated limits, is directly proportional to the carrier density, the resonance strength is also directly proportional to the carrier density. When the resonance-field position is directly proportional to frequency, as is the case for all magnetic resonances under discussion, $\tilde{\kappa}_m''$ is inversely proportional to frequency, resulting in the resonance strength being proportional to the square of the frequency.

C. Magnetic resonances in EHD in Ge

As in the case of radius-independent electric resonances, graphical presentations of the real part of the principal dielectric tensor elements κ_m' are useful in identifying the field positions of magnetic resonances. The intersection of the real part of one principal dielectric tensor element with the negative of the real part of another, selected in accordance with the requirements of the resonance conditions (48) and (49), pinpoints the fields at which the various resonances occur. Figure 8 presents such graphs for the situation where $\vec{B}$ is parallel to the [100] crystallographic axis of Ge. The intersections accurately locate the field positions of the resonances in the power absorption spectra shown in Fig. 9 [except for the resonances marked 1, 4, and 8, which occur at the electron–cyclotron-resonance field in the three polarizations and do not correspond to the resonance conditions (48) and (49)].

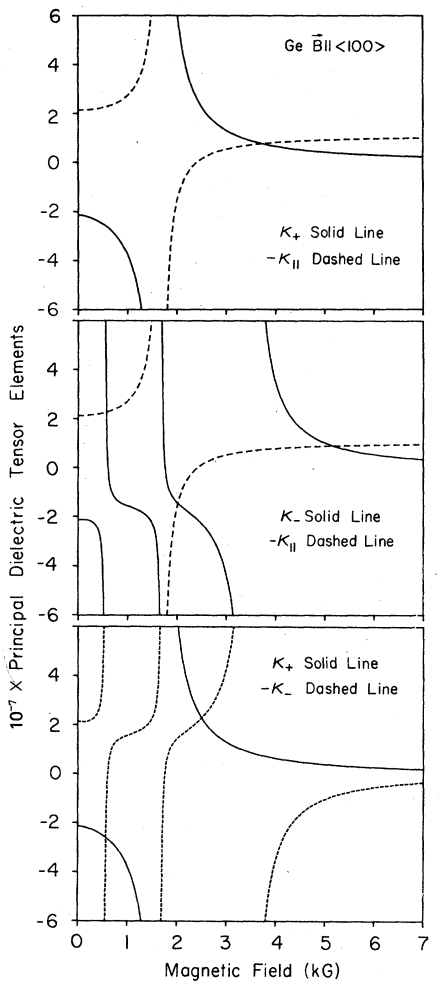

FIG. 8. Principal dielectric tensor elements in the lossless limit as a function of magnetic field for Ge with $\vec{B}$ parallel to the [100] axis. The material parameters used in these calculations are identical to those listed in the caption of Fig. 1. The intersection of a dielectric tensor element with the negative of another pinpoints the location of all the magnetic resonances shown in Fig. 9 except those at the electron–cyclotron-resonance field.

Each singularity in the lossless expressions for $\kappa_{\pm}'$ has associated with it one particular resonance, occurring in the transverse circular polarization corresponding to the dielectric tensor element which has the singularity. In the high-carrier-density region (κ_l ignored), each resonance occurs at one to three times the cyclotron-resonance field of the carrier with which the singularity is connected. We recall that, for an isotropic single-

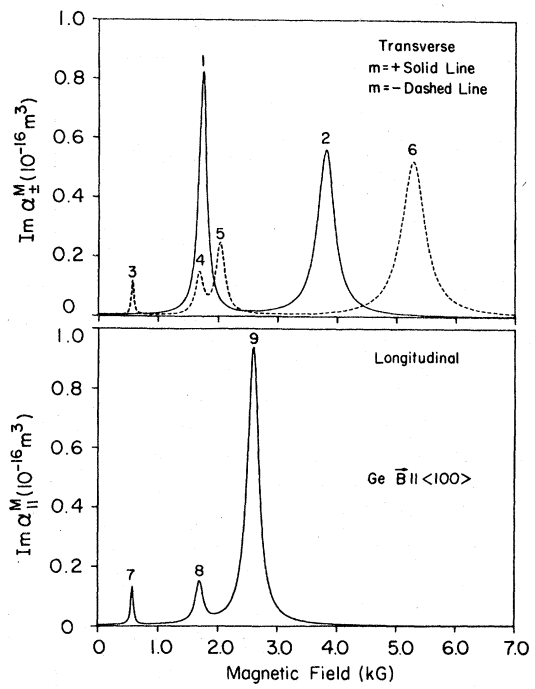

FIG. 9. Imaginary part of the magnetic polarizability for the three modes of excitation of a 3-μm-radius gyrotropic sphere as a function of magnetic field for Ge with $\vec{B}$ aligned along the [100] axis. The sphere parameters are given in the caption of Fig. 2.

carrier system, a single resonance existed which occurred at exactly twice the cyclotron-resonance field of the carrier in the CRA polarization. Thus, in Fig. 9, resonance 3 is associated with light holes and resonance 6, with heavy holes. Resonance 2 is associated with the singularity in the (+) polarization connected with the presence of the electrons. Resonance 5 is linked to the singularity in the (−) polarization resulting from the anisotropy of the electron band structure.

Resonances 7 and 9, in the longitudinal polarization, are hybrid resonances, having the same general character as the isotropic two-carrier longitudinal resonance described by the resonance condition (56). The field position of resonance 7 is determined mainly by light hole and electron effective masses and the ratio of the concentration of light holes to the concentration of electrons, while the position of resonance 9 is determined mostly by the heavy hole and electron effective masses and the ratio of the density of heavy holes to the density of electrons. Specifically, employing resonance condition (49) in the lossless limit, neglecting κ_I, i.e., assuming $\omega_{pe} \gg \sqrt{\kappa_I}\,\omega$, and ignoring one hole band, we find that

$$B_{\parallel}^{\mathrm{res}} = \frac{\omega}{e}\left(M_h M_1 \frac{M_h + r_h M_{pe}}{r_h M_h + M_1}\right)^{1/2}, \tag{58}$$

where $r_h = n_h/n$. In the case of heavy holes (resonance 9), $r_{\mathrm{hh}} \simeq 1$ and $M_{pe}/M_1 \simeq 0.8$ so that

$$B_{\parallel}^{\mathrm{res}} \simeq (\omega/e)(M_{\mathrm{hh}} M_1)^{1/2}. \tag{59}$$

And, in the case of light holes (resonance 7), $r_{\mathrm{lh}} \simeq 0$ so that

$$B_{\parallel}^{\mathrm{res}} \simeq (\omega/e) M_{\mathrm{lh}}. \tag{60}$$

All six of these resonances have resonance fields proportional to frequency and independent of carrier concentration (see Fig. 10) in the high-concentration limit (which is applicable for EHD parameters), in which κ_l can be ignored. Consequently, as previously mentioned, their resonance strengths are directly proportional to n and vary as the square of frequency and fifth power of radius. In the low-carrier limit or cyclotron-resonance regime, the resonance positions are again inde-

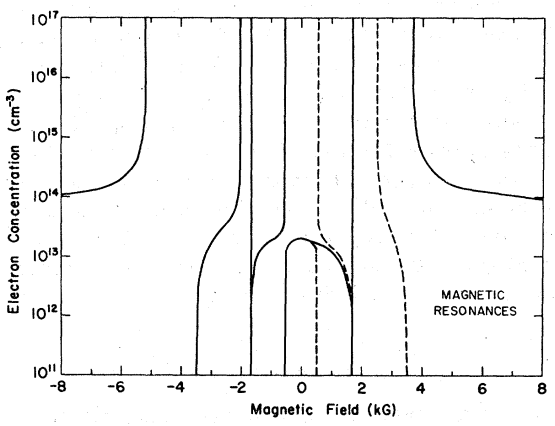

FIG. 10. Field positions of the magnetic resonances as a function of carrier concentration for the case of a 1-μm-radius magnetoplasma sphere with $\vec{B}$ parallel to the [100] axis in Ge. The material parameters used are described in the caption of Fig. 3. The resonances in the (−) circular polarization are plotted on the negative side of the field axis. The positions of the resonances in the transverse polarization are plotted with solid lines while the positions of the longitudinal resonances are plotted with dashed lines. Note that, as in the case of the electric resonances, there are two regions where the resonance positions are independent of carrier concentration: the high-carrier-concentration regime ($n > 2\times10^{14}$ cm^{-3}) and the low-carrier-concentration regime ($n < 2\times10^{13}$ cm^{-3}). Note that the unscreened resonances, located at the electron–cyclotron-resonance field in all three polarizations, remain fixed in position independent of carrier density.

pendent of carrier concentration, being fixed at the cyclotron-resonance fields of the carriers (see Fig. 10).

Resonances 1, 4, and 8 are all located at the electron-cyclotron-resonance field, $B_{ce}=M_{ce}\omega/e$; and, in the high-carrier-density regime, their resonance strengths show the same dependence on radius, carrier concentration, and frequency as the other six resonances. These three resonances exist because of the simultaneous "blowup" of κ_+, κ_-, and $\kappa_\parallel$, resulting from the anisotropy of the electron-band structure. The mechanism by which these resonances are produced is best understood by examining the internal fields, which we do below.

In the case of the magnetic polarizability discussed by FFW,[10] the permeability of the medium outside the sphere and the permeability of the sphere material itself are both assumed to be equal to that of free space; i.e., all the media under consideration are assumed to be nonmagnetic. The equality of the permeabilities of the two media results in the elimination of the very type of term (the zero-order term in FFW) which dominates the electric polarizability in the Rayleigh limit.[31] Consequently, the internal electric, magnetic, and total current fields associated with the magnetic interaction are not uniform across the interior of the sphere, as happens for the electric interaction.

The power is absorbed by the sphere from the external time-varying magnetic field via the internal electric field induced by the magnetic field. The mean power absorbed by the sphere is given by

$$P_m^M=\tfrac{1}{2}\,\mathrm{Re}\left(\int_V \vec{j}_m^{\,\mathrm{int}}\cdot\vec{E}_m^{\,\mathrm{int}*}\,dV\right)$$
$$=\tfrac{1}{2}\,\mathrm{Re}\left(\int_V \vec{J}_m^{\,\mathrm{int}}\cdot\vec{E}_m^{\,\mathrm{int}*}\,dV\right), \qquad (61)$$

where $\vec{J}_m^{\,\mathrm{int}}$ is the internal total current density, the sum of the conduction and displacement current densities, as defined in Eq. (2) of Ref. 10, and the volume integral is over the sphere volume. In the limit we are discussing, in which the radius-dependent correction terms in the magnetic polarizability are neglected so that α_m^M is defined by Eq. (46), the first-order terms in the perturbation expansion are adequate for the calculation of the absorbed power. That is,

$$P_m^M=\tfrac{1}{2}\,\mathrm{Re}\left(\int_V \vec{J}_m^{(1)}\cdot\vec{E}_m^{(1)*}dV\right), \qquad (62)$$

where $\vec{J}_m^{(1)}$, defined by Eq.(30) of Ref. 10, is

$$\vec{J}_m^{(1)}=\omega^2\epsilon_0\tilde{\kappa}_m|\vec{B}_m^{\mathrm{ac}}|\hat{e}_m\times\vec{r}, \qquad (63)$$

$\vec{E}_m^{(1)}$, which is related to $\vec{J}_m^{(1)}$ via the generalized Hall-Ohm law, Eq. (7) of Ref. 10, is

$$\vec{E}_m^{(1)}=\omega|\vec{B}_m^{\mathrm{ac}}|\begin{cases}\dfrac{-\kappa_\parallel}{\kappa_m+\kappa_\parallel}\,z\hat{e}_m\pm\dfrac{\kappa_m}{\kappa_m+\kappa_\parallel}\,\dfrac{x\pm iy}{\sqrt{2}}\,\hat{e}_\parallel & (m=\pm)\\ \dfrac{\kappa_-}{\kappa_++\kappa_-}\,(x-iy)\hat{e}_+-\dfrac{\kappa_+}{\kappa_++\kappa_-}\,(x+iy)\hat{e}_- & (m=\|),\end{cases} \qquad (64)$$

and the origin of the coordinate system is at the center of the sphere.

As the cyclotron-resonance field of an isotropic carrier is neared, $|\kappa_m|\to\infty$, where $m=+$ or $-$, according to the sign of the carrier. But, since $\kappa_\parallel$ and κ_{-m} do not also approach infinity simultaneously with κ_m, the component of the electric field $\vec{E}_m^{(1)}$ with the proper polarization $\hat{e}_m$ to interact with the cyclotron motion of the carrier is suppressed and only the noninteracting polarizations remain. Thus, in the case of isotropic carriers, no resonances appear at the cyclotron-resonance fields of the carriers because of the screening of the CRA component of the internal electric field by the free carriers. However, in the case of a carrier with an anisotropic band structure, $|\kappa_+|$, $|\kappa_-|$, and $|\kappa_\parallel|$ all approach infinity simultaneously. The quantities $\kappa_\parallel/(\kappa_m+\kappa_\parallel)$ and $\kappa_m/(\kappa_++\kappa_-)$ appearing in Eq.

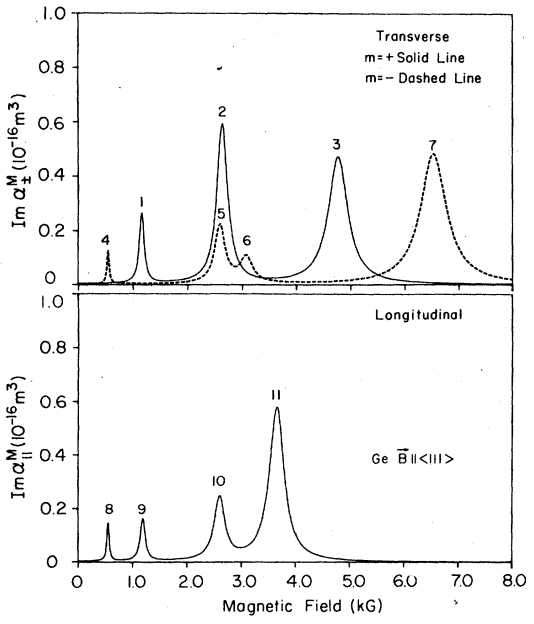

FIG. 11. Imaginary part of the polarizability for the three modes of excitation of a 3-μm-radius gyrotropic sphere as a function of magnetic field for Ge with $\vec{B}$ aligned along the [111] axis. The sphere parameters are described in the caption of Fig. 6.

(64) do not then approach zero. Thus, at the cyclotron-resonance field of a carrier with an anisotropic band structure, the component of the internal electric field which can couple to the cyclotron motion of the carrier is not screened out. Resonances 1, 4, and 8 in Fig. 9 are, therefore, the result of incomplete screening.[24]

Equation (64) also elucidates the nature of the remaining resonances (marked 2, 3, 5, 6, 7, 9). They are associated with an internal field "blowup," occurring at the resonance conditions (48) and (49), as can be seen from the denominator in $\vec{E}_m^{(1)}$. This behavior is analogous to that responsible for the origin of the electric resonances (see Fig. 5).

When the dc magnetic field is aligned along the [111] crystallographic axis in Ge, eleven resonances, two more than exist in the [100] case, appear in the spectra, as shown in Fig. 11. The two additional resonances are associated with the inequivalence of the ellipsoids in the electron-band structure when the magnetic field is aligned along the [111] direction.

IV. DISCUSSION

If we assume a plane-wave relationship between the incident external electric and magnetic fields, the relative strengths of the electric and magnetic resonances are given by the relative magnitudes of the imaginary parts of the electric and magnetic polarizabilities divided by $\sqrt{\kappa_0}$. At 35 GHz for compensated EHD magnetoplasma spheres with radii of 3 μm, the magnetic resonances are roughly two orders of magnitude stronger than the electric resonances. Because of the different dependence of resonance strength on radius for the two types of resonances, the magnetic resonances are expected to be even more important for larger radii while the electric resonances are expected to dominate for smaller drops. Also, as a function of frequency, the strengths of the electric resonances will grow more rapidly (as ω^4) than will the strengths of the magnetic resonances (as ω^2). At submillimeter wavelengths for typical EHD parameters, the two types of resonances will be of the same order of magnitude in strength.

For a compensated EHD magnetoplasma sphere at microwave or far-infrared frequencies, the field positions of all resonances, both electric and magnetic, are functions only of the carrier effective masses and the population ratio of heavy holes to electrons and of light holes to electrons. Consequently, the resonances are particularly well suited for the measurement of the effective masses of the carriers within the drop. However, in doped Ge, where the EHD magnetoplasma can be uncompensated, there are resonances available which are sensitive to both the total carrier concentration and the degree to which the magnetoplasma is uncompensated.

Finally, there has been difficulty in interpreting experimental microwave and far-infrared spectra in terms of EHD resonances and resonances of the free-carrier gas surrounding the drops. Our results point to the importance of using separate normal-mode excitations in carrying out such experiments, e.g., use of circular polarizations rather than linear polarizations[3] in the situation where the time-varying fields are perpendicular to $\vec{B}$, to aid in the identification of these highly complex resonances.

In summary, we have presented a description of the interaction of time-varying electric and magnetic fields with a spherical EHD magnetoplasma in the context of the Drude model. However, as previously mentioned, the FFW macroscopic formalism used in our discussion can be employed with any local-limit model for the gyrotropic dielectric tensor. Thus our treatment of EHD can be suitably modified to incorporate a whole host of field-dependent features of EHD (e.g., quantum oscillations of the free-carrier concentration) which we have ignored by use of the simple Drude model.

ACKNOWLEDGMENT

The authors gratefully acknowledge the support of the NSF MRL Program No. DMR76-00889A1.

---

*Present address: Thomas More College, P. O. Box 85, Ft. Mitchell, Ky. 41017.

[1]K. Fujii and E. Otsuka, J. Phys. Soc. Jpn. 38, 742 (1975).

[2]B. M. Ashkinadze and P. D. Altukhov, Fiz. Tverd. Tela 17, 1004 (1975) [Sov. Phys. Solid State 17, 643 (1975)].

[3]V. I. Gavrilenko, V. L. Kononenko, T. S. Mandel'shtam, and V. N. Murzin, Dokl. Akad. Nauk SSSR 232, 802 (1977) [Sov. Phys. Dokl. 22, 82 (1977)]; Pis'ma Zh. Eskp. Teor. Fiz. 23, 701 (1976) [JETP Lett. 23, 645 (1976)].

[4]K. Muro and Y. Nisida, J. Phys. Soc. Jpn. 40, 1069 (1976).

[5]P. G. Baranov, Yu. P. Veshchunov, R. A. Zhitnikov, N. G. Romanov, and Yu. G. Shreter, Pis'ma Zh. Eskp. Teor. Fiz 26, 369 (1977) [JETP Lett. 26, 249 (1977)].

[6]R. S. Markiewicz, J. P. Wolfe, and C. D. Jeffries, Phys. Rev. Lett. 32, 1357 (1974); 34, 59 (E) (1975).

[7]J. P. Wolfe, R. S. Markiewicz, C. Kittel, and C. D. Jeffries, Phys. Rev. Lett. 34, 275 (1975).

[8]M. Cardona and B. Rosenblum, Phys. Rev. 129, 991 (1963).
[9]H. Numata, J. Phys. Soc. Jpn. 36, 309 (1974).
[10]G. W. Ford, J. K. Furdyna, and S. A. Werner, Phys. Rev. B 12, 1452 (1975).
[11]The smallness criteria, for which FFW theory is valid, are $(\omega/c)a \ll 1$ and $a^2(\omega/c)^2 \left| (\kappa_{xx}^2 + \kappa_{xy}^2)/\kappa_{xx} \right| \ll 1$, where ω is the signal frequency and a is the radius of the sphere.
[12]We assume that small EHD are spherical in shape in the presence of a dc magnetic field even though small EHD may be distorted in a magnetic field {see V. L. Kononenko, Fiz. Tverd. Tela 19, 3010 (1977) [Sov. Phys. Solid State 19, 1762 (1977)] and V. L. Kononenko and V. N. Murzin, Pis'ma Zh. Eksp. Teor. Fiz. 24, 590 (1976) [JETP Lett. 24, 548 (1976)]}. We note that magnetostriction of large EHD (γ drops) has been observed via vidicon imaging experiments by J. P. Wolfe, J. E. Furneaux, and R. S. Markiewicz, in *Proceedings of the Thirteenth International Conference on the Physics of Semiconductors*, edited by F. G. Fumi (North-Holland, Amsterdam, 1976), p. 954; J. P. Wolfe, R. S. Markiewicz, J. E. Furneaux, S. M. Kelso, and C. D. Jeffries, Phys. Status Solidi B 83, 305 (1977); H. L. Stormer and D. Bimberg, Commun. Phys. 1, 131 (1976).
[13]M. Voos, K. L. Shaklee, and J. M. Worlock, Phys. Rev. Lett. 33, 1161 (1974).
[14]J. M. Worlock, T. C. Damen, K. L. Shaklee, and J. P. Gordon, Phys. Rev. Lett. 33, 771 (1974).
[15]Ya. E. Pokrovskii and K. I. Svistunova, Fiz. Tekh. Poluprovodn. 4, 491 (1970) [Sov. Phys. Semicond. 4, 409]; Pis'ma Zh. Eksp. Teor. Fiz. 13, 297 (1971) [JETP Lett. 13, 212 (1971)]; V. M. Asnin, A. A. Rogachev, and N. I. Sablina, Fiz. Tverd. Tela 14, 399 (1972) [Sov. Phys. Solid State 14, 332 (1972)]; C. Benoit à la Guillaume, M. Voos, F. Salvan, J. M. Laurant, and A. Bonnot, C. R. Acad. Sci. Ser. B 272, 236 (1971); J. M. Hvam and O. Christensen, Solid State Commun. 15 929 (1974).
[16]F. L. Galeener, Phys. Rev. Lett. 22, 1292 (1969); Ph.D. thesis (Purdue University, 1970) (unpublished).
[17]L. D. Landau and E. M. Lifshitz, *Electrodynamics of Continuous Media* (Addison-Wesley, Reading, Mass., 1960), p. 300.
[18]G. Dresselhaus, A. Kip, and C. Kittel, Phys. Rev. 100, 618 (1955).
[19]V. L. Kononenko, Fiz. Tverd. Tela 17, 3264 (1975) [Sov. Phys. Solid State 17, 2146 (1975)].
[20]E. D. Palik and J. K. Furdyna, Rep. Prog. Phys. 33, 1193 (1970).
[21]We do not consider the possible renormalization of the carrier effective masses in the EHD discussed by T. M. Rice, Nuovo Cimento B 23, 226 (1974) and J. C. Hensel, T. G. Phillips, and G. A. Thomas, in *Solid State Physics*, Vol. 32, edited by H. Ehrenreich, F F. Seitz, and D. Turnbull (Academic, New York, 1977), p. 87.
[22]W. B. Levinger and D. R. Frankl, J. Phys. Chem. Solids 20, 281 (1961).
[23]J. C. Hensel and K. Suzuki, Phys. Rev. B 9, 4219 (1974).
[24]G. E. Smith, L. C. Hebel, and S. J. Buchsbaum, Phys. Rev. 129, 154 (1963).
[25]J. R. Dixon and J. K. Furdyna, in *Proceedings of the 13th International Conference on the Physics of Semiconductors*, edited by F. G. Fumi (North-Holland, Amsterdam, 1976), p. 918.
[26]Ya. E. Pokrovskii and K. I. Svistunova, in *Proceedings of the 12th International Conference on the Physics of Semiconductors* (Teubner, Stuttgart, 1974), p. 71.
[27]Ya. E. Pokrovskii and K. I. Svistunova, Pis'ma Zh. Eksp. Teor. Fiz. 19, 92 (1974) [JETP Lett. 19, 56 (1974)].
[28]R. E. Halliwell and R. R. Parsons, Can. J. Phys. 52, 1336 (1974).
[29]Radius-dependent resonances were discussed in the context of the FFW perturbation theory by J. R. Dixon and J. K. Furdyna, Phys. Rev. B 13, 4626 (1976); 14, 2698 (E) (1976). A discussion of radius-dependent resonances in the context of the general solution to the gyrotropic sphere problem is presented in G. W. Ford and S. A. Werner, Phys. Rev. B 18, 6752 (1978), and J. R. Dixon and J. K. Furdyna, *ibid.* 18, 6770 (1978).
[30]T. A. Evans and J. K. Furdyna, Phys. Rev. B 8, 1461 (1973).
[31]R. S. Brazis and J. K. Furdyna, Phys. Rev. B 16, 3273 (1977).